Proceedings of the 6th International Conference on Computing and Data Science
DOI: 10.54254/2755-2721/68/20241441

Analysis of multi-UAV communication networking problem in constrained geographic environments based on improved simulated annealing optimization algorithm

Zhennan Ma

Institute of Smart City and Intelligent Transportation, Southwest Jiaotong University, Chengdu, China

2577630164@qq.com

Abstract. This paper conducts an in-depth exploration of UAV communication networking and path planning within geographically constrained environments. The study begins with necessary data preprocessing, which includes the conversion of latitude and longitude coordinates and the organization of antenna parameters. Through the development of a model based on coordinate geometry, this research effectively identifies communication blind spots and establishes a comprehensive geometric envelope for signal coverage. To enhance network efficiency and path planning, the paper introduces a hybrid optimization algorithm that combines simulated annealing and genetic algorithms. Simulated annealing is used to optimize the selection of communication types between network nodes, while genetic algorithms refine the UAV fleet's flight routes based on these communication strategies. This dual-layered approach allows for fine-tuned adjustments in response to dynamic environmental constraints. The effectiveness of this method is demonstrated through simulations, which reveal a communication coverage rate of 73.7272%. These results confirm that the proposed hybrid optimization technique significantly improves both communication coverage and operational efficiency of UAV networks in complex environments. This provides substantial theoretical insights and practical contributions to the field of UAV network optimization, which is particularly valuable for applications in remote or urban areas where geographical constraints pose significant challenges.

Keywords: Path Planning, Simulated Annealing Algorithm, Genetic Algorithm, UAV Communication Networking, Rasterization.

1. Introduction

In contemporary research, the application of Unmanned Aerial Vehicles (UAVs) has significantly expanded across various fields, including maritime operations, agriculture, rescue, and surveillance. Particularly under geographically constrained conditions, such as areas with significant altitude variations, the construction of communication networks and path planning for UAVs become crucial. These geographic limitations, especially at flight altitudes of 3km, greatly affect the efficiency of UAV communications and the safety of mission execution.

As discussed by Nomikos et al., UAV-assisted maritime communications need to overcome numerous deployment and environmental challenges, especially in complex maritime geographic settings [1]. Additionally, Aggarwal and Kumar reviewed various technologies and challenges

DOI: 10.54254/2755-2721/68/20241441

associated with UAV path planning under terrain constraints, emphasizing the importance of efficient path planning in maintaining communication stability and avoiding terrain obstacles[2].

This paper aims to optimize the communication network and path planning for UAVs in high-altitude areas by integrating improved simulated annealing and genetic algorithms. Considering Ding Lu-fei's analysis of omnidirectional antennas as ideal "point sources," we assume optimal communication is achievable without obstructions [3]. Moreover, we refer to Yan et al.'s research on path planning in complex 3D environments and Zhu et al.'s analysis of the performance of short-wave communications [4][8].

Through the integration and simulation of these critical technologies, this study not only provides new strategies for deploying UAVs in terrain-complex areas but also validates the effectiveness and practicality of the proposed methods through empirical research. By ensuring precise path planning and effective communication strategies, our research contributes to enhancing the operational efficiency and safety of UAVs in high-altitude regions, thus offering theoretical and practical guidance for future UAV applications.

2. Literature Review

2.1. UAV Communication in Challenging Environments

Unmanned Aerial Vehicles (UAVs) have increasingly been utilized for communication purposes, especially in maritime and geographically constrained environments. The deployment of UAVs in these areas involves complex considerations, including the establishment of reliable communication links in the presence of natural and human-made obstructions [1][2]. The increasing dependency on UAVs for critical tasks underlines the importance of robust communication networks, which must be optimized to ensure continuous service and coverage in varied terrains and conditions.

2.2. Path Planning for UAVs

Path planning remains a significant challenge for UAVs, especially when operating in constrained or hazardous environments. Techniques for UAV path planning have evolved, addressing both the efficiency of the route and the safety of the aerial vehicles. Aggarwal and Kumar highlighted several strategies that have been developed to navigate these challenges, offering solutions and identifying ongoing challenges in this domain [2]. Effective path planning is essential not only for the optimization of routes but also for minimizing potential disruptions in UAV communications.

2.3. Theoretical Foundations in UAV Communication Networking

The principles of radar technology are fundamental in determining the parameters for antenna operations and by extension, the communication strategies of UAV networks. These principles assume that antennas function as ideal point sources, which simplifies the analysis and modeling of UAV communication systems [3]. This theoretical foundation supports the development of algorithms tailored to optimize communication paths and network efficiency in constrained environments.[4]

2.4. Optimization Algorithms in UAV Networking

To address the complexities of UAV path planning and network optimization, researchers have turned to advanced algorithmic approaches. Hybrid optimization techniques, which combine genetic algorithms and simulated annealing, have shown promise in refining UAV communication networks. These algorithms offer a robust framework for making dynamic adjustments in real-time, enhancing the operational efficiency and coverage of UAV fleets in challenging environments [13][14]. The genetic algorithm, in particular, has been noted for its potential to fall into local optima, which is a significant consideration when designing these systems [12].

DOI: 10.54254/2755-2721/68/20241441

2.5. Modeling and Simulation Challenges

The adaptation of UAV networks to real-world geographic constraints requires accurate modeling and simulation. Techniques such as the use of digital elevation models (DEMs) have been instrumental in converting geographical data into formats that can be used for effective simulation and planning [5][6]. Furthermore, the complexity of modeling in 3D environments has led researchers to develop coordinate geometry-based models, which facilitate the identification and analysis of communication blind spots in UAV networks [4].

2.6. Future Directions and Challenges

The literature on UAV communication networking highlights a range of strategies and technologies developed to address the challenges of operating in constrained geographic environments. The theoretical and practical contributions of these studies provide a solid foundation for further innovation and optimization of UAV networks [11]. As UAV technologies continue to evolve, the integration of more sophisticated optimization algorithms and modeling techniques will be crucial. The application of algorithms such as DBSCAN for identifying communication blockages and the use of probabilistic roadmaps for complex 3D environments represent the forefront of research in this area [9][10]. These advancements are expected to drive significant improvements in UAV communication networks, particularly in terms of efficiency, reliability, and adaptability to environmental constraints.

3. Methodology

3.1. Antenna Operating Parameters

To reduce the complexity of planning and to highlight the constraints of geographic environments, the antennas used in UAV communication in this paper are set as omnidirectional antennas, unlike those shown in Figure 1 where some antennas in space have stronger transmission power in certain directions. In this case, the feed source can be considered as an ideal "point source" for analysis, and its radiation pattern is shown in Figure 2[3].

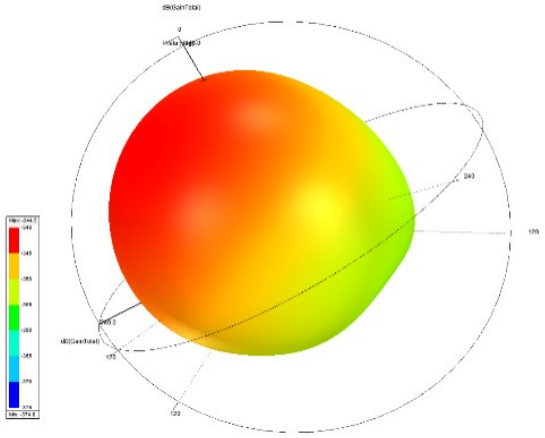

Figure 1. gain diagram of a single polarized antenna

DOI: 10.54254/2755-2721/68/20241441

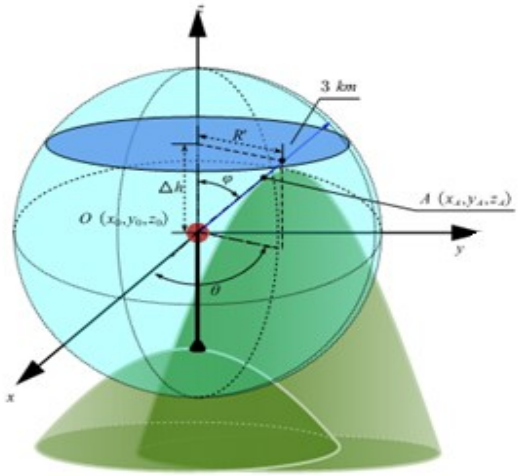

Figure 2. diagram of antenna microwave radiation

As antennas function as reciprocal systems, their transmission and reception are fundamentally consistent, thus it can be considered that antennas are capable of receiving microwaves from "all space." Moreover, the method for calculating the maximum communication distance ***d*** is[8]:

$$20\lg d(km) = P_T(dBm) - P_R(dBm) + 20\lg \mu - 32.44 - 20\lg f(MHz) \tag{3.1}$$

In this formula, $P_T(dBm)$ represents the transmission power, $P_R(dBm)$ represents the receiver sensitivity, μ is the attenuation factor of the propagation medium, and $f(MHz)$ is the frequency.

3.2. Latitude and Longitude Grid Conversion

The Digital Elevation Model (DEM) is a digital representation of the surface topography, containing rich geomorphological information essential for geoscientific application analysis [5][6]. It is noted that Attachment 2 presents the elevation conditions of various regions, and uses the method of "initial latitude and longitude"and"DEM grid size ***d***" for positioning. Considering that subsequent needs require converting the measurement units from "degrees" to "meters," this section discusses how to process the existing data.

For ease of analysis, this paper first assumes the Earth as a standard sphere with a radius R, thus the circumference of the Earth is approximately $2\pi R$ meters. Since the length of Earth's meridians is essentially constant, moving 1 meter in the north-south direction corresponds to a fixed degree change in latitude [4]:

$$\Delta B = \frac{360^o}{2\pi R}$$

The length of Earth's parallels (latitude lines) varies with latitude. Therefore, moving 1 meter in the east-west direction corresponds to a change in longitude given by [4]:

$$\Delta L = \frac{360^o}{2\pi R \cos B}$$

where L and B are the longitude and latitude of the location, respectively. Within the range of an individual communication site, the effect of Earth's curvature can essentially be ignored, making it more convenient to use "meters" as the unit of measurement for positioning [6]. However, the relative positions of different communication sites are characterized by latitude and longitude coordinates. Therefore, it is necessary to utilize ΔB and ΔL to modify the formula for the distance between two points on a plane [5]:

DOI: 10.54254/2755-2721/68/20241441

$$S = 2\arcsin\sqrt{\sin^2\frac{B_1 - B_2}{2} + \cos B_1 \cos B_2 + \sin^2\frac{L_1 - L_2}{2}} \times R \tag{3.2}$$

From formula (5.2), it is possible to achieve antenna positioning in full space, thereby integrating communication sites using the same communication methods into the same space on a unified scale. The integration schematic is shown in Figure 3.

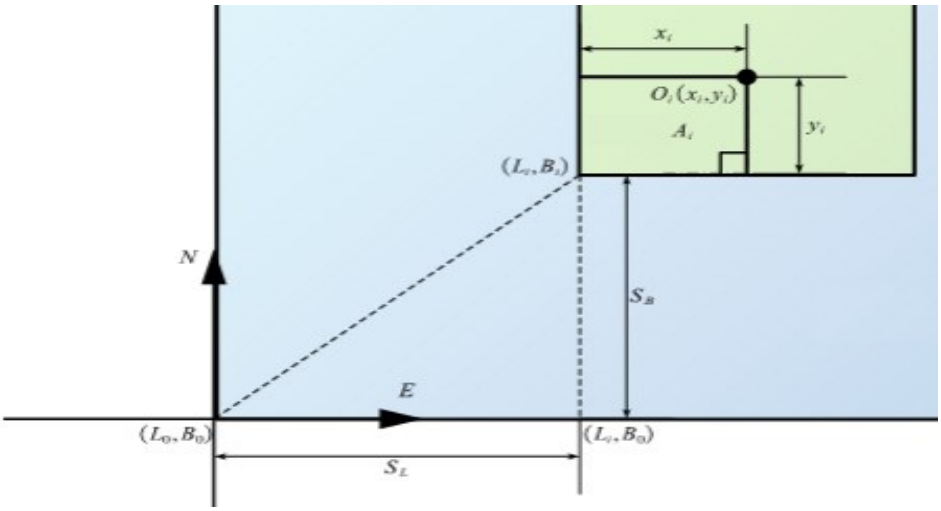

Figure 3. Schematic Diagram of Latitude and Longitude Grid Positioning

3.3. Construction of a Communication Blind Spot Location Model Based on Coordinate Geometry

3.3.1. Communication boundary analysis. After initial screening, it is known that the height of the antenna feed source is significantly less than 3 km. Therefore, within a 3 km airspace, there are no large mountains causing signal area blockages, representing a strictly simply connected plane. Hence, there is only one scenario for communication disruption [3]—the signal radiated outward from the feed source encounters obstacles such as mountains during its journey to the 3 km airspace. To determine the boundaries of communication, it is necessary to analyze the tangency situations between the radiation lines and the obstacles [4]:

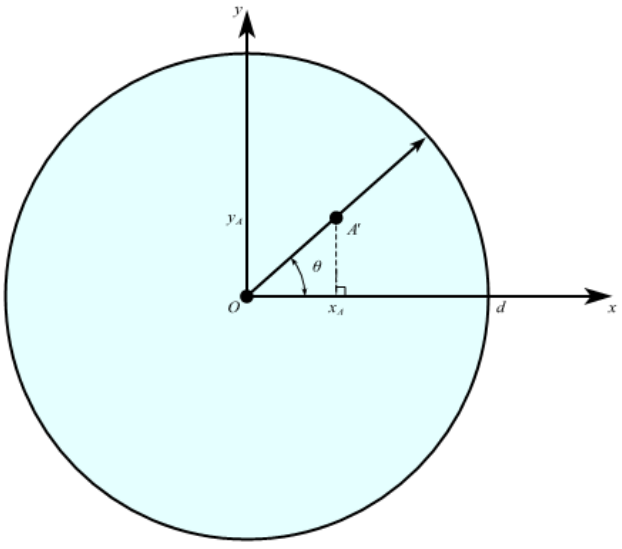

Figure 4. Schematic Diagram of Microwave Radiation Projection

DOI: 10.54254/2755-2721/68/20241441

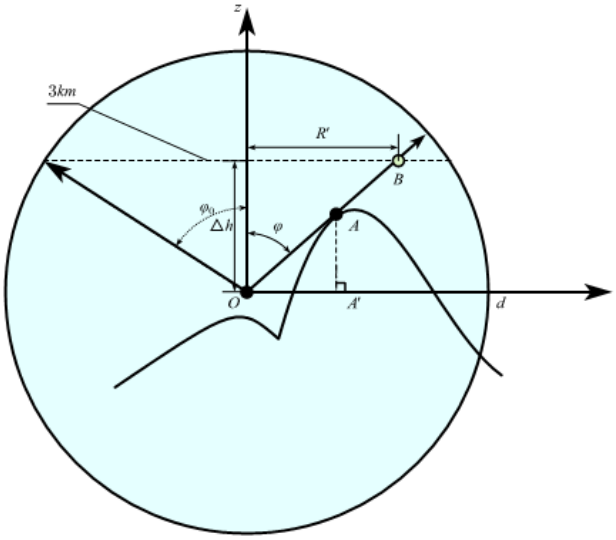

Figure 5. Cross-Sectional Diagram of Microwave Radiation

Select a point A (x_A, y_A, z_A) on the surface of an obstacle where the feed source ray is tangent. Project point A onto the XOY plane to get point A' (as shown in Figure 4). Record the angle θ between vector $\overrightarrow{OA'}$ and the x-axis. The calculation method is as follows:

$$\theta = \arccos\left(\frac{\hat{e}_x \cdot \overrightarrow{OA'}}{\overrightarrow{OA'}}\right) = \arccos\left(\frac{|x_A - x_0|}{\sqrt{(x_A - x_0)^2 + (y_A + y_0)^2}}\right) \tag{3.3}$$

Where $\hat{e}_x$ is the unit vector in the direction of the x-axis; the plane formed by vector $\overrightarrow{OA'}$ and the z-axis includes the emission situation of the ray (in an ideal model). This paper uses the direction of $\overrightarrow{OA'}$ as the positive direction of the horizontal axis, and the direction away from the ground as the positive direction of the vertical axis. The cross-section shown in the figure is drawn accordingly.

3.3.2. Construction of a Coordinate Model for Line-of-Sight Communication Boundaries with Omnidirectional Direct Wave Antennas. Spatial Constraint 1: The above analysis has detailed the principle of determining communication boundaries on a specific cross-section. Furthermore, this paper formulates it into a mathematical form suitable for computation. Assuming the communication area m utilizes communication methods D_j ,the corresponding ideal 3 km airspace communication circle radius R_j is calculated as: $R_j = \sqrt{d_j^2 - \Delta h_m^2}$ [7].If any point $P(x_i, y_i, b_{m_{ij}})$ within the current area can obstruct communication, as can be easily understood from the projection diagram (Figure 4):

$$\sqrt{(x_A - x_0)^2 + (y_A + y_0)^2} < R_j \tag{3.4}$$

Spatial Constraint 2: Further, this paper notes that point P needs to be located within a conical space, which has the antenna feed source $O(x_0, y_0, z_0)$ as the apex and the ideal 3 km airspace communication circle as the base, fulfilling $\varphi_i < \varphi_0$ where:

DOI: 10.54254/2755-2721/68/20241441

$$\varphi_i = \arccos\left(\frac{|z_i - z_0|}{\sqrt{(x_i - x_0)^2 + (y_i - y_0)^2 + (z_i - z_0)^2}}\right) < \frac{\Delta h_m}{d_j} \tag{3.5}$$

Δh_m is the vertical distance between the antenna feed source O in communication area m and the 3 km airspace.$d_j$represents the maximum ground-to-air communication distance for the communication means D_j [8].

Taking the case where $x_i > x_0, y_i > y_0$ as an example, and considering $z_k = 3000$, the line-of-sight communication boundary coordinate model for an omnidirectional direct wave antenna and its spatial constraints are as follows:

$$\begin{cases} x_k = x_0 \pm \Delta h_m \cos\theta_i \tan\varphi_i \\ y_k = y_0 \pm \Delta h_m \cos\theta_i \tan\varphi_i \end{cases}$$

$$s.t. \begin{cases} \Delta h_m = 3000 - b_{m_{ij}} - h_m \\ \frac{y_i}{x_i} = \frac{y_k}{x_k} = tan\,\theta_i \\ cos\,\theta_i = \frac{|x_i - x_0|}{\sqrt{(x_i - x_0)^2 + (y_i - y_0)^2}} \\ \varphi_i = arccos\left(\frac{|z_i - z_0|}{\sqrt{(x_i - x_0)^2 + (y_i - y_0)^2 + (z_i - z_0)^2}}\right) \\ \varphi_i < \frac{\Delta h_m}{d_j} \\ \sqrt{(x_A - x_0)^2 + (y_A + y_0)^2} < R_j \end{cases} \tag{3.6}$$

In this context, $Q(x_k, y_k, z_k)$ represents a communication blocking point within the 3 km airspace that needs to be identified, while $P(x_i, y_i, b_{m_{ij}})$ are points within region *m* that obstruct communication. The height of the antenna in region *m* is denoted by Δh_m ,and represents the vertical distance from the antenna feed source in region *m* to the 3 km airspace. The angles φ_i and θ_i are the azimuth angles of points Q and P in the spherical coordinate system, respectively. The termd_j refers to the maximum ground-to-air communication distance for the communication means D_j [8].

To determine the area covered by the signal within the 3 km airspace, this paper calculates the ideal communication circle radius in the 3 km airspace, R_j, as follows: $R_j = \sqrt{d_j^2 - \Delta h_m^2}$. Subtracting from this the impact of model (3.6), the resultant area is the ideal signal coverage area. This calculation takes into account the maximum communication distance d_j for each communication method D_j, adjusted for the vertical distance Δh_m from the antenna feed source to the 3 km airspace. The result provides a precise estimation of the region effectively covered by the signal, considering both horizontal reach and vertical elevation constraints.

3.4. Rasterization Processing and Flight Parameter Calibration

In UAV swarm path planning models, two common methods are used to represent the paths: a time series composed of flight speed and heading [10], and a time series made up of spatial position coordinates [2]. To calculate a flight path that meets specified constraints, the flying area is divided into M×N grids of equal size. According to relevant literature, it can be stipulated[4] that when UAVs move in the four cardinal directions—east, south, west, and north—each movement is counted as one unit of

DOI: 10.54254/2755-2721/68/20241441

length. However, when moving in the diagonal directions—southeast, northeast, southwest, and northwest—each movement is counted as $\sqrt{2}$ units of length.

This paper constructs a UAV swarm mission completion flight planning model [11] based on this search space, resulting in an optimal flight route for the UAV swarm based on geometry. Each UAV movement is from the center of one grid to the center of an adjacent grid. Ignoring the effects of the latitude and longitude grid and the Earth's curvature, the UAVs' discretized coordinates are defined as:

$$\{(x,y)\,|\,0 \le x < N, 0 \le y < M; x, y \in Z\} \tag{3.7}$$

3.5. Construction of UAV Swarm Flight Path Planning Model

The research objective of this paper is the path planning for multi-UAV multi-target communication coordination, thus the core is a multi-objective optimization problem. By adjusting the overall flight paths of the UAVs, the goals are to minimize communication blind spots [11] and reduce flight distances [13]. This chapter focuses on discussing how to perform dimensionality reduction on multiple objectives and determine the existing conditional constraints for each objective, ultimately constructing a flight path planning model.

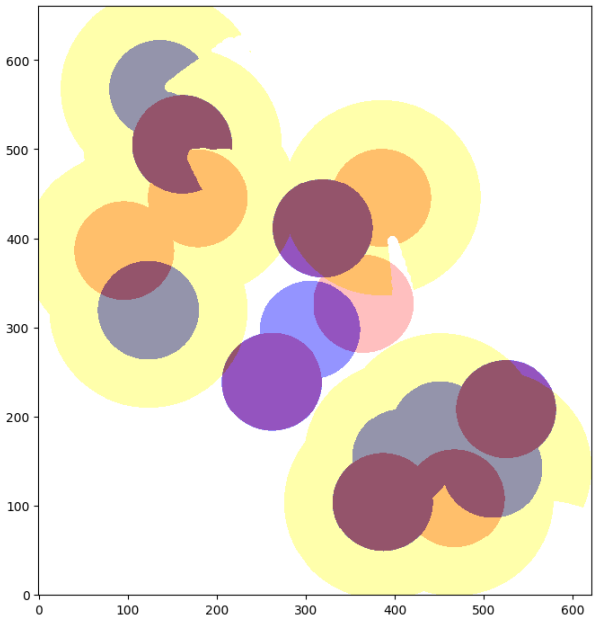

Figure 6. Schematic of Full Communication Coverage Before Grid Processing

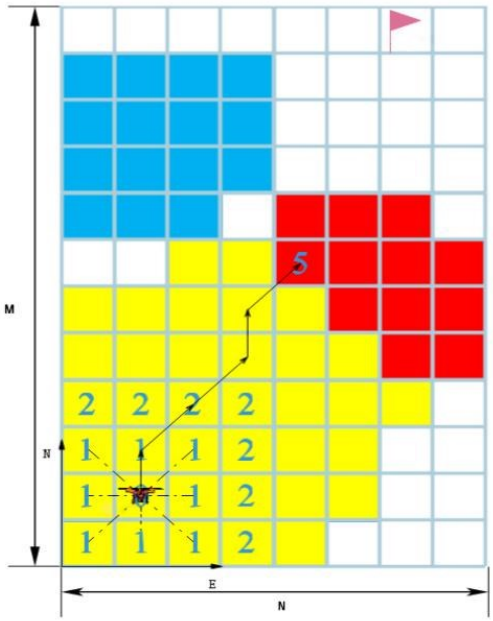

Figure 7. Schematic of Grid Processing

3.5.1. Decision Variables. Multi-objective optimization problems typically require dimensionality reduction by transforming multiple objectives into a single objective for resolution. Given that there are distinct priorities among the three decision-making objectives [11], this paper considers conducting a weight analysis on the three indicators to achieve dimensionality reduction. Based on this method, the paper further proposes the following requirements for constructing the indicators:

1.The direction of the indicators should be consistent, meaning that for the ultimate optimization goal, they should all be either positive or negative indicators.

2.The scale of the indicators should be as uniform as possible to facilitate the reflection of weight differences.

Communication Blind Spot Indicator (T): As explained in section 3.4, each UAV movement can mark the current moving grid as well as the total moving grids. Therefore, this paper attempts to

DOI: 10.54254/2755-2721/68/20241441

construct the "Minimum Communication Blind Spots" indicator by counting the total number of grids traversed by the UAVs' movement paths and the number of communication blind spots encountered:

$$T = 1 - \frac{\sum_{i=1}^{n}\sum_{k=1}^{n_i} d_{ik_0}}{\sum_{i=1}^{n} n_i}, n_i \in Z \tag{3.8}$$

$$d_{ik_0} = \begin{cases} 1, (\mathrm{E_{ik}}, \mathrm{N_{ik}}) \text{ to the i-th UAV whose its k-th move is a communication blind spot.} \\ 0, (\mathrm{E_{ik}}, \mathrm{N_{ik}}) \text{ to the i-th UAV, whose k-th move is a non-communication blind spot.} \end{cases}$$

Where n_i represents the total number of grids moved by the i-th UAV.

Flight Distance Indicator (H): As detailed in section 3.4, since each move involves only one grid and the coordinates after rasterization comply with the distance calculation formula in a Cartesian coordinate system, the construction approach for the "Minimum Flight Distance" indicator is derived by referring to the construction plan used for the communication blind spot indicator [4]:

$$H = \frac{\sum_{i=1}^{n} m_i}{\sum_{i=1}^{n}\sum_{k=1}^{n_i}\sqrt{(E_{ik} - E_{i(k-1)})^2 + (N_{ik} - N_{i(k-1)})^2}}; E_{ik}, N_{ik} \in Z$$

$$m_i = \sqrt{(E_{if} - E_{i0})^2 + (N_{if} - N_{i0})^2} \tag{3.9}$$

$(\mathrm{E_{ik}}, \mathrm{N_{ik}})$ represents the coordinates of the grid to which the i-th UAV moves on its k-th move, with $(\mathrm{E_{i0}}, \mathrm{N_{i0}})$ being the starting point and $(\mathrm{E_{if}}, \mathrm{N_{if}})$ being the endpoint. Therefore, m_i is the ideal shortest distance for the i-th UAV.

In summary, this paper has constructed mathematical indicators for three optimization objectives. For the final path planning, both indicators are positive, and the range of variation for all three indicators is [0,1]. Therefore, weights are assigned to the communication blind spot indicator (T) and the flight distance indicator (H) as follows [10]:

$$\omega_T = \frac{2}{3}, \omega_H = \frac{1}{3} \tag{3.10}$$

Further, in combination with section 3.4 regarding the regulations for flight paths, further explanations are needed to translate these into mathematical form as constraint conditions.

3.5.2. Constraint Conditions. Drone swarm path planning is usually subject to the movement limitations of the drones themselves, environmental restrictions, and coordination constraints between different drones. Based on this, this paper establishes the following constraint conditions:

Self-imposed constraints: Due to the drone having only eight possible directions of movement, and the step length of each move limiting its speed, the following constraints apply to the movement of an individual drone:

DOI: 10.54254/2755-2721/68/20241441

$$\begin{cases} 0 \le \left| E_{ik} - E_{i(k-1)} \right| \le 1 \\ 0 \le \left| N_{ik} - N_{i(k-1)} \right| \le 1 \\ E_{ik}, N_{ik} \in Z \\ k = 1,2,3,...,n_i \\ i = 1,2,3,...,n \end{cases} \tag{3.11}$$

Environmental constraints: In the context of this problem, drones cannot exceed a 3km airspace defined by an MxN gridded area. Therefore, the grid coordinates of the drones (E_{ik}, N_{ik}) are subject to the following constraints:

$$\begin{cases} 0 \le E_{ik} < M \\ 0 \le N_{ik} < N \end{cases} \tag{3.12}$$

Coordination constraints: Although in this paper the path planning for the drone swarm is simplified to a non-temporal geometric problem, to some extent ignoring the spatial coordination issues that arise when three drones arrive at the same grid simultaneously, it is necessary to avoid drones falling into a cycle of ineffective searching, which could prevent other drones from planning their paths. Therefore, a maximum range for the number of grid moves must be set, namely a temporal coordination constraint:

$$0 \le n_i < M \times N, i = 1,2,3,....,n \tag{3.13}$$

3.5.3. Objective Function. By constructing optimization objectives and conducting multi-objective dimensionality reduction analysis, this paper has developed the objective function ultimately used for calculating the effectiveness of flight route planning:

$$J = \omega_T T + \omega_H H \tag{3.14}$$

This paper designs the sum of weights to equal 1, allowing the proportion of weights for each indicator to be clearly reflected in the objective function. By combining the limitations of the magnitude of each indicator, it achieves control over the scale of computation.

3.5.4. Optimal Model for Drone Swarm Flight Path Planning. From objective function (3.14), it is apparent that the optimal flight path for multiple drones to complete the mission requires the optimization objective J to be maximized as much as possible. Therefore, the optimization objective is:

$$\max_{s.t.} J = \omega_T T + \omega_H H \tag{3.15}$$

Combining the constraint conditions analyzed above, this paper has developed the following optimal model for drone swarm flight path planning:

$$\max_{s.t.} J = \omega_T T + \omega_H H = \frac{2\sum_{i=1}^{n} m_i}{3\sum_{i=1}^{n}\sum_{k=1}^{n_i}\sqrt{(E_{ik} - E_{i(k-1)})^2 + (N_{ik} - N_{i(k-1)})^2}} + \frac{\sqrt{(E_{if} - E_{i0})^2 + (N_{if} - N_{i0})^2}}{3}$$

$$s.t. \begin{cases} 0 \le \left| E_{ik} - E_{i(k-1)} \right| \le 1 \\ 0 \le \left| N_{ik} - N_{i(k-1)} \right| \le 1 \\ 0 \le E_{ik} < M \\ 0 \le N_{ik} < N \\ 0 \le n_i < M \times N \\ E_{ik}, N_{ik} \in Z \\ k = 1,2,3,...,n_i \\ i = 1,2,3,...,n \end{cases} \tag{3.16}$$

DOI: 10.54254/2755-2721/68/20241441

Based on this, the paper designs an algorithm to solve the composite path optimization model for a formation of drones.

3.6. Design of a Combined Optimization Algorithm Based on Improved Simulated Annealing and Genetic Algorithm

This problem, as an optimal path issue, involves dynamic optimization, combinatorial optimization, and multi-objective optimization; the variety of combinations is complex, and conventional heuristic algorithms tend to be insufficient. It is necessary to design algorithms layer by layer for each optimization objective of this problem to explore the optimal feasible solution. The genetic algorithm, as a heuristic stochastic search algorithm that mimics natural laws, can achieve global searching by simulating key operations such as selection [12], crossover, and mutation, thereby obtaining the optimal solution to the problem. However, it is prone to premature convergence [11], easily reaching local optima, thus necessitating the combination with other algorithms for evaluating the solution. Therefore, this paper chooses to use the simulated annealing algorithm to generate relatively inferior optimal solutions externally [13][14], thereby avoiding the genetic algorithm falling into local optima; meanwhile, the internal genetic algorithm somewhat speeds up the original temperature decline process, significantly shortening the optimization time [13], and allows for a relatively lower initial temperature to be used in iterations, further shortening the decay time.

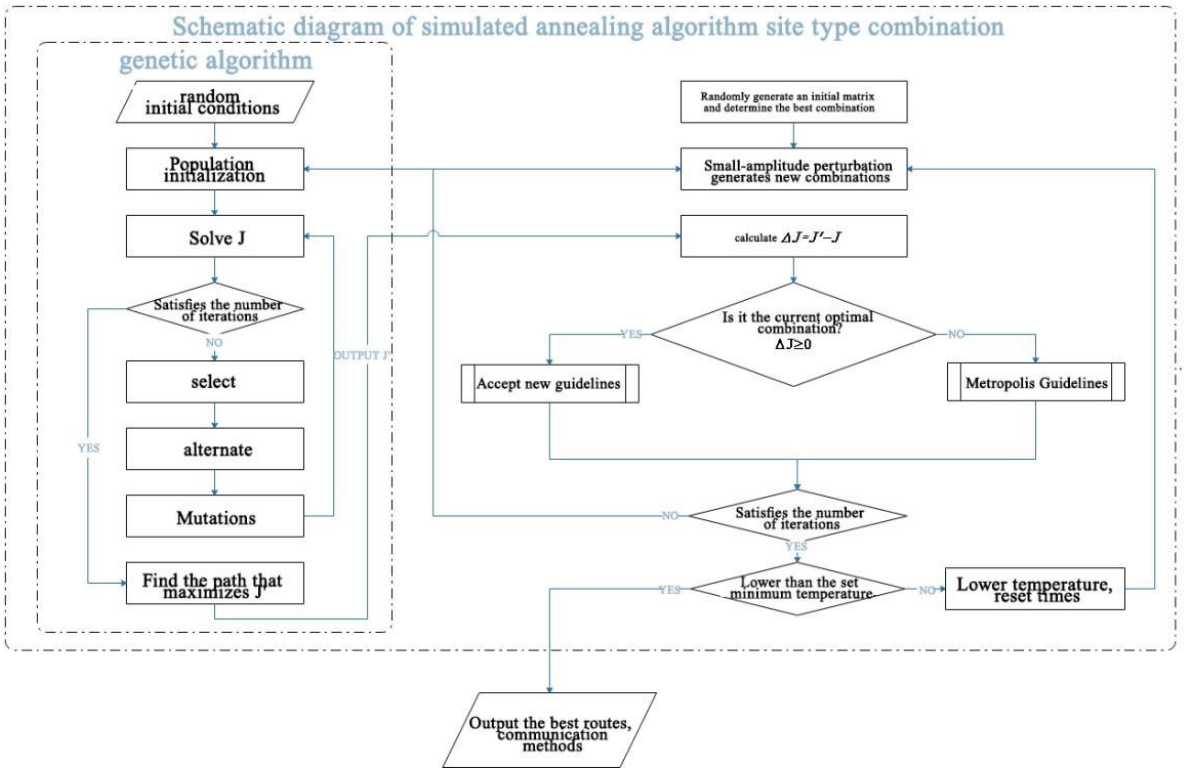

Figure 8. Improved simulated annealing combination optimization algorithm flow char

Based on the above analysis and in conjunction with the model context, this paper attempts to design an improved combined optimization algorithm of simulated annealing-genetic algorithm (see flowchart in Figure 6): The outer layer of the algorithm follows the simulated annealing method to update the communication method matrix for site types, ultimately obtaining the optimal combination of communication methods for the sites; the inner layer of the genetic algorithm solves for fitness based on model (3.15), thereby obtaining the optimal flight route under the current communication combination.

DOI: 10.54254/2755-2721/68/20241441

4. Results

For the verification of the model results, this paper chooses the method of simulation. Sixteen different sites are selected (locations shown in Figure 6), and three drones transmitting different signals are set (see Table 1). The solution process is as follows.

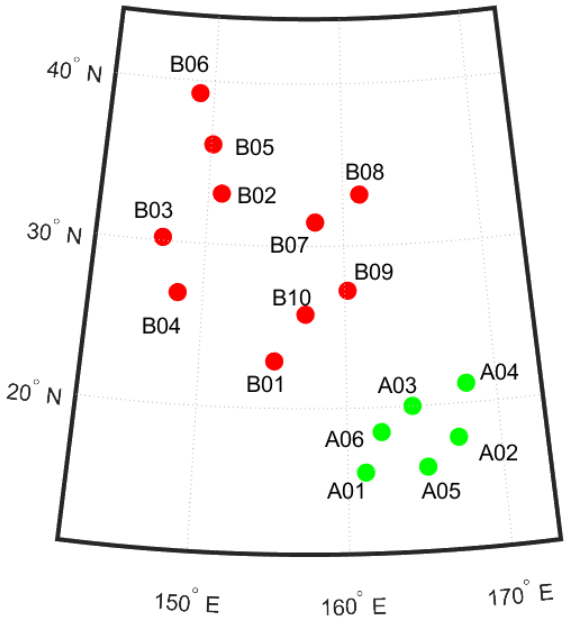

Figure 9. Site Location Map

Table 1. UAV grouping information table

Drone Type	Flight Altitude (km)	Starting Position	Endpoint (Target Area Position)	Communication Method
Drone A	3	N 15.1241° E 160.774°	N 42.4523° E 143.3121°	D1/D2
Drone B	3	N 33.1537° E 161.2351°	N 43.6294° E 142.7564°	D1/D3
Drone C	3	N 20.1932° E 168.7678°	N 43.1342° E 143.1324°	D1

4.1. Integrated Solution for Communication Blockage Areas Based on Clustering-Convex Hull Algorithm

This section will specifically elaborate on how to use clustering algorithms to integrate communication blockage points in a 3km airspace, while utilizing the convex hull algorithm to outline the boundaries, thus achieving pixel segmentation of the communication area. The technical roadmap is as follows:

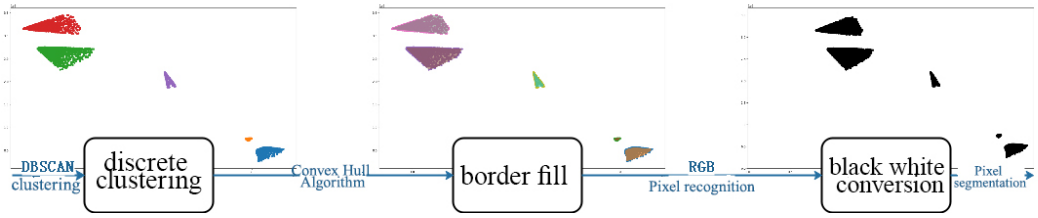

Figure 10. technical roadmap

DOI: 10.54254/2755-2721/68/20241441

Based on the above algorithms, this paper identifies the communication blockage domains for three different communication methods. Due to the complex colors of the blockage domains after clustering-convex hull processing, this paper uniformly converts them into black and white images (see Figure 9) to facilitate the subsequent transformation of result formats.

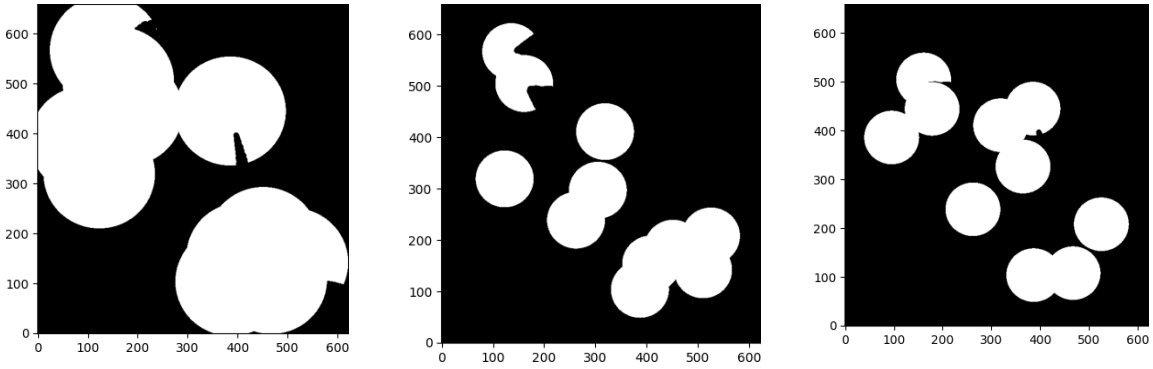

(a):D1 (b):D2 (c):D3

Figure 11. 3km Communication Coverage Envelope Network

Finally, information on drone formations after gridding can be obtained (see Table 2).

Table 2. after gridding UAV grouping information table

Drone Type	Starting Grid Coordinates (Ei0, Ni0)	Ending Grid Coordinates (Eif, Nif)	Communication Method
Drone A	(378, 82)	(26, 629)	D1, D2
Drone B	(385, 443)	(15, 653)	D1, D3
Drone C	(535, 184)	(23, 643)	D1

4.2. Solution of Combined Optimization Algorithm Based on Simulated Annealing and Genetic Algorithm

4.2.1. Optimal Flight Route Solution Based on Genetic Algorithm. As the inner algorithm of the combined optimization algorithm in this paper, the genetic algorithm receives the 'communication map' information provided by the outer simulated annealing layer [11]. It optimizes the flight routes of drones on this 'map', repeatedly iterates multiple times, stores the currently optimal path, and feeds back the maximum fitness $\boldsymbol{J'}$ to the simulated annealing (Figure 12,13).

DOI: 10.54254/2755-2721/68/20241441

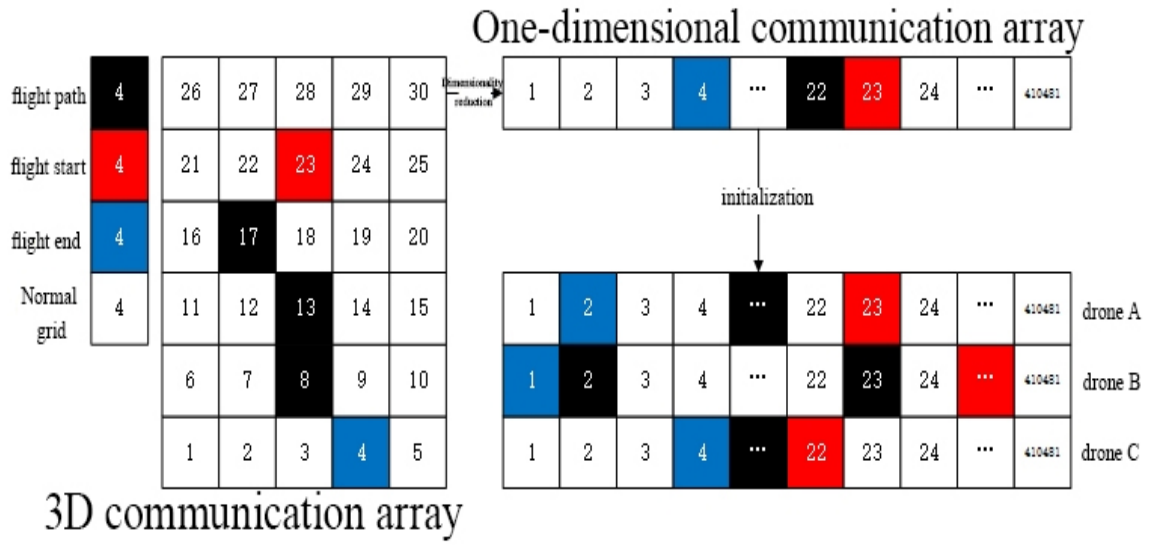

Figure 12. Schematic Diagram of Communication Map Dimension Reduction and Population Initialization

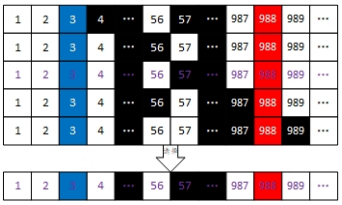

Figure 13. Selection

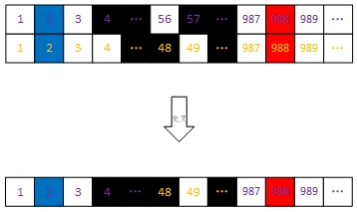

Figure 14. Crossover

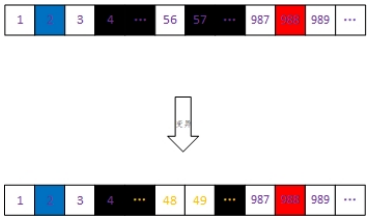

Figure 15. Mutation

By mimicking the mechanisms of selection and genetics in nature to find the optimal solution, it is possible to avoid the algorithm getting trapped in local optima to some extent[12]. This paper, through multiple iterations and repeating the above operations, determines the maximum fitness of the current population and the corresponding optimal flight route. The former is input into the outer layer of simulated annealing for further solution, which is discussed in detail as follows.

4.2.2. Solution for the Optimal Communication Combination Using the Improved Simulated Annealing Algorithm. From the above text, it is known that this paper has obtained the maximum fitness J′under the given communication combination through an improved genetic algorithm. This section focuses on discussing the algorithm details of the outer layer of simulated annealing, which receives the fitness J, modifies the communication combination, and feeds it back to the inner layer of the genetic algorithm.

The Simulated Annealing algorithm (SA) simulates the annealing process of solid materials, gradually transforming the system from a high-energy state to a low-energy state through heating and cooling. In the problem-solving process, the solution corresponds to the particle states within the solid, and the objective function corresponds to the particle's energy [13]. The simulated annealing algorithm has good local search capabilities but does not have a comprehensive understanding of the entire search space. Therefore, combining the genetic algorithm with the simulated annealing algorithm can better solve the problem [14]. It can avoid falling into local optima and also improve search efficiency.

4.3. Simulation Solution Results

According to the above process, the planning results for the simulation problem can be obtained, with the site allocation results shown in Table 3, and the drone path planning results shown in Figure 16.

DOI: 10.54254/2755-2721/68/20241441

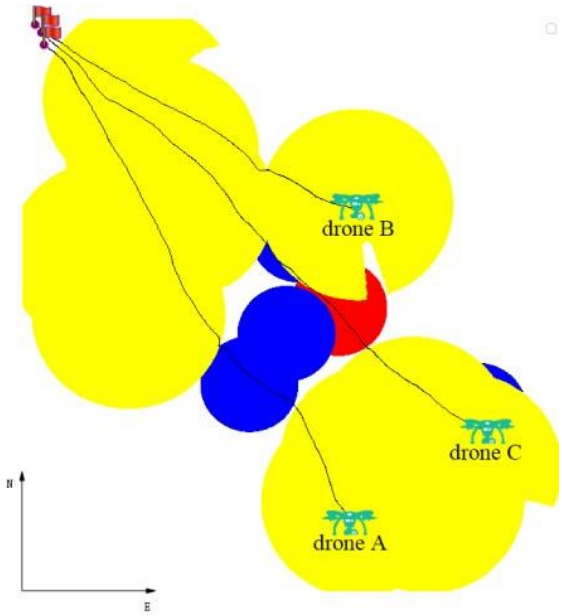

Figure 16. Optimal Flight Route Planning Results

Table 3. Site Type Allocation table

Site Type	D1	D2	D3
A01	B03	A04	B09
A02	B04	B01	
A03	B05	B07	
A05	B06	B10	
A06	B08		
B02			

5. Discussion

5.1. Model Solution and Analysis

This paper identifies and marks the grid coordinates that a drone swarm passes through during flight using a combined optimization algorithm, and these are plotted into the planned routes shown in Figure 17. In the figure, the yellow area represents the D1 communication coverage area, the blue area represents the D2 communication coverage area, and the red area represents the D3 communication coverage area.

Comprehensive analysis reveals that the flight paths of the three drones are generally aligned with the direction connecting their start and end points. Regarding communication blind spots, drones commonly leave the communication area radially and similarly enter the next communication area from a blind spot radially, consistent with real communication scenarios. The blind spots before the endpoint generally affect all three drones, and compared to Drones A and B, Drone C has a larger range of communication blind spots on its flight path, which could be considered for future optimization.

DOI: 10.54254/2755-2721/68/20241441

Combining the above optimization needs, this paper has calculated a communication coverage rate of 73.7272% under the current planning conditions, successfully achieving the goal of path optimization.

6. Conclusions

The clustering drone route planning problem is a complex combinatorial optimization problem, and traditional methods may struggle to find the optimal solution. However, this paper combines genetic algorithms and simulated annealing algorithms to effectively search the solution space, making it more likely to find better solutions [10]. Moreover, genetic algorithms and simulated annealing algorithms both have flexibility and robustness, allowing them to handle different types of optimization problems, and they are less likely to get trapped in local optima compared to some local search methods.

However, this paper simplifies the model by ignoring the curvature of the Earth and using image recognition technology to grid the target airspace [1], which reduces the accuracy of the model solution to some extent [7]. In the future, it may be possible to improve the accuracy of drone positioning and route planning strategies by using latitude and longitude calculations.

The model established in this paper has strong generality and applicability, and can be applied to optimization problems in many different fields. Similar to the problem of clustering drone route planning, the logistics and transportation industry also faces challenges in optimizing route planning to minimize costs or maximize efficiency [2]. Additionally, the model construction and algorithm design approach in this paper can be used to optimize delivery routes, vehicle scheduling, warehouse layout, and other problems in logistics and transportation. Moreover, it can also be applied to reducing costs in fields such as power and energy management, communication networks, manufacturing, and production.

References

[1] N. Nomikos, P. K. Gkonis, P. S. Bithas and P. Trakadas, "A Survey on UAV-Aided Maritime Communications: Deployment Considerations, Applications, and Future Challenges," in IEEE Open Journal of the Communications Society, vol. 4, pp. 56-78, 2023

[2] Aggarwal S, Kumar N. Path planning techniques for unmanned aerial vehicles: A review, solutions, and challenges[J]. Computer communications, 2020, 149: 270-299

[3] DING Lu-fei. Principles of radar[M]. Third Ed. Xi'an: Xi'an Electronic Sience &Technology University Press, 2006

[4] F YAN, Y S Liu and J Z. Xiao, "Path planning in complex 3D environments using a probabilistic roadmap method[J]", International Journal of Automation and Computing, vol. 10, no. 6, pp. 525-533, 2013

[5] LI Zhuang-zhi, ZHANG You-sai. Simulation of landform echo wave based on DEM[J]. Computer Simulation, 2007, 24(5): 176-178

[6] SONG Jia. Researh on automated relief form types classification of China based on DEM[D]. Xi'an: Northwest University, 2006

[7] IN Kefan, WANG Hongdong, YI Hong, LIU Jingyang, WANG Jian. Key technologies and intelligence evolution of maritime UV[J]. Chinese Journal of Ship Research, 2018, 13(6): 1-8

[8] X. Zhu, "Short Wave Communication Transmission Signal Monitoring Method based on Genetic Algorithm," 2021 Second International Conference on Electronics and Sustainable Communication Systems (ICESC), Coimbatore, India, 2021, pp. 1041-1044

[9] H. V. Singh, A. Girdhar and S. Dahiya, "A Literature survey based on DBSCAN algorithms," 2022 6th International Conference on Intelligent Computing and Control Systems (ICICCS), Madurai, India, 2022, pp. 751-758

[10] Z. He and L. Zhao, "The Comparison of Four UAV Path Planning Algorithms Based on Geometry Search Algorithm," 2017 9th International Conference on Intelligent Human-Machine Systems and Cybernetics (IHMSC), Hangzhou, China, 2017, pp. 33-36

[11] CAO Y, WEI W, BAI Y, et al. Multi-base multi-uav cooperative reconnaissance path planning with genetic algorithm[J]. Cluster Computing, 2019, 22: 5175-5184

DOI: 10.54254/2755-2721/68/20241441

[12] A. Lambora, K. Gupta and K. Chopra, "Genetic Algorithm- A Literature Review," 2019 International Conference on Machine Learning, Big Data, Cloud and Parallel Computing (COMITCon), Faridabad, India, 2019, pp. 380-384
[13] X. Yue and W. Zhang, "UAV Path Planning Based on K-Means Algorithm and Simulated Annealing Algorithm," 2018 37th Chinese Control Conference (CCC), Wuhan, China, 2018
[14] T. Turker, O. K. Sahingoz and G. Yilmaz, "2D path planning for UAVs in radar threatening environment using simulated annealing algorithm," 2015 International Conference on Unmanned Aircraft Systems (ICUAS), Denver, CO, USA, 2015